A Novel Stochastic Slow Frequency Hopping Simulation Model for Rayleigh Fading Channels

Conference Paper · September 2001

2 authors, including:

A Novel Stochastic Slow Frequency Hopping Simulation Model for Rayleigh Fading Channels

Cheng-Xiang Wang and Matthias Pätzold

Department of Communication Networks, Technical University of Hamburg-Harburg
Denickestr. 17, D-21071 Hamburg, Germany
chengxiang.wang@tu-harburg.de

Abstract

We propose a novel stochastic slow frequency hopping simulation model for Rayleigh fading channels, which is very useful for investigating the problems of stationary or slowly moving mobile stations being subjected to prolonged deep fades in the GSM system. Closed-form expressions are provided for all parameters of the simulation model. Furthermore, the performance of the proposed channel simulator is investigated for typical frequency hopping mobile radio data transmission scenarios. Numerical results show that the proposed channel simulator has excellent frequency hopping capabilities and its statistical correlation properties are in very good conformity with the underlying physical radio channel model.

Keywords

Rayleigh fading channels, stochastic simulation models, slow frequency hopping, statistics.

1. Introduction

Frequency hopping (FH), which is well known as one of the efficient techniques in combating channel fading, has been the subject of considerable research effort in recent years. First of all, we must differentiate between "fast" and "slow" frequency hopping techniques. Fast frequency hopping (FFH), in which the operating frequency is changed many times per symbol, has widely been used in spread-spectrum multiple access (SSMA) systems [1]–[6] and Bluetooth wireless networks [7] because of its excellent anti-interference properties. On the other hand, slow frequency hopping (SFH), which is of primary interest in this paper, has been proposed for various narrow-band TDMA systems, including the GSM Pan-European System [8]. It is so called because the operating frequency is changed only once per TDMA frame [9]. FH reduces the signal-to-noise ratio required for good communications and adds frequency diversity to the channel [10], because "hopping" over several frequencies randomizes the occurrence of fades.

Simulation models for mobile fading channels are important for the design, performance evaluation, optimization, and test of modern wireless communication systems. A SFH channel simulator, which models accurately the physical channel statistics determined by cyclic or pseudo-random hopping patterns of the carrier frequency, is extremely useful for the investigation of the problems of stationary or slowly moving mobile stations being subjected to prolonged deep fades in the GSM system. In recent years, several channels models with FH capabilities have been developed. For example, a variable data rate FH channel model has been derived by using frequency transform techniques and digital filter design methods in [11], and a method of generating correlated multipath fading in order to emulate FH in a wide-band channel has been described in [12], only to mention a few.

In this paper, a novel SFH GSM channel simulator for Rayleigh fading channels is proposed. Due to its high flexibility, the simulation model enables a better statistical fitting to physical radio channel model than other channel models, such as the model introduced in [13]. Our model is based on a finite sum of weighted harmonic functions with determined frequencies (Rice's sum of sinusoids) [14, 15] and takes into account that the fading envelope of two different frequency-spaced channels is in general correlated.

2. The theoretical reference model and its correlation properties

In this section, we briefly describe the reference model, which is important when discussing the performance and correlation properties of our stochastic simulation model in Section 4.

Without any loss of generality, we restrict our investigations to frequency non-selective fading channels, where the coherence bandwidth of the channel is large in comparison to the bandwidth of the transmitted signal, and we describe the channel model by making use of the equivalent complex baseband notation. For simplicity, we assume that no line-of-sight path exists between the base station and the mobile station antennas. Then, the envelope of the received signals at two different carrier frequencies, denoted by F_1 and F_2, can be modelled by the following Rayleigh processes:

$$\zeta(t) = |\mu_1(t) + j\mu_2(t)| \,, \text{ at } F_1 \,, \tag{1a}$$

$$\zeta'(t) = |\mu_1'(t) + j\mu_2'(t)| \,, \text{ at } F_2 \,, \tag{1b}$$

where both $\mu_i(t)$ and $\mu_i'(t)$ $(i = 1, 2)$ are real Gaussian noise processes, each with zero mean and variance σ_0^2. The existence of different time delays over the propagation paths causes the statistical properties of two signals with different frequencies to become essentially uncorrelated if the absolute value of the frequency separation $\chi = F_2 - F_1$ is sufficiently large. Here, χ is a measure for a frequency hop from F_1 to F_2. But in general, the received signals $\zeta(t)$ and $\zeta'(t)$ are statistically correlated due to the limited bandwidth available for the GSM system. For example, the uplink transmissions are carried out in the 890–915 MHz band, where the maximum relative hopping frequency is $25\text{MHz}/900\text{MHz} \approx 2.8\%$ [8].

The statistics and correlation properties of two signals received at F_1 and F_2 are completely determined by the correlation properties of the underlying Gaussian noise processes $\mu_i(t)$ and $\mu_j'(t)$ $(i, j = 1, 2)$. Therefore, we can restrict our investigations to the following autocorrelation and cross-correlation

functions:

$$r_{\mu_i\mu_j}(\tau) := E\{\mu_i(t)\mu_j(t+\tau)\} ,\qquad(2a)$$

$$r_{\mu_i\mu_j'}(\tau,\chi) := E\{\mu_i(t)\mu_j'(t+\tau)\} ,\qquad(2b)$$

for all $i = 1,2$ and $j = 1,2$, where the operator $E\{\cdot\}$ refers to statistical average. It should be observed that (2b) is a function of both time separation τ and frequency separation χ. The statistical properties of interest can be derived provided that the horizontal directivity pattern of the receiving antenna and the angular distribution of the incident power are known [16]. On the assumption that the antenna is omnidirectional and the angle of arrival is uniformly distributed, the expressions (2a) and (2b) can be solved analytically [16, p. 51]:

$$r_{\mu_1\mu_1}(\tau) = r_{\mu_2\mu_2}(\tau) = \sigma_0^2 J_0(2\pi f_{max}\tau) ,\qquad(3a)$$

$$r_{\mu_1\mu_2}(\tau) = r_{\mu_1'\mu_2'}(\tau) = 0 ,\qquad(3b)$$

$$r_{\mu_1\mu_1'}(\tau,\chi) = r_{\mu_2\mu_2'}(\tau,\chi) = \frac{\sigma_0^2 J_0(2\pi f_{max}\tau)}{1 + (2\pi\alpha\chi)^2} ,\qquad(3c)$$

$$r_{\mu_1\mu_2'}(\tau,\chi) = -r_{\mu_2\mu_1'}(\tau,\chi) = -2\pi\alpha\chi r_{\mu_1\mu_1'}(\tau,\chi) ,\qquad(3d)$$

where α is related to the delay spread and f_{max} is the maximum Doppler frequency. The above expressions provide the basis for the performance evaluation of our stochastic simulation model in Section 4.

3. Description of the SFH simulation model

In this section, we propose a novel stochastic SFH Rayleigh fading channel simulator by making use of the fact that the real Gaussian noise processes $\mu_i(t)$ and $\mu_i'(t)$ [see (1a) and (1b), respectively] can be modelled by a finite sum of properly weighted sinusoids [17]:

$$\hat{\mu}_1(t) = \sum_{n=-N+1}^{N}\sum_{m=1}^{M} c_{n,m}\cos(2\pi f_n t - \theta_m - \hat{\theta}_m) ,\quad(4a)$$

$$\hat{\mu}_2(t) = \sum_{n=-N+1}^{N}\sum_{m=1}^{M} c_{n,m}\sin(2\pi f_n t - \theta_m - \hat{\theta}_m) ,\quad(4b)$$

$$\hat{\mu}_1'(t) = \sum_{n=-N+1}^{N}\sum_{m=1}^{M} c_{n,m}\cos(2\pi f_n t - \theta_m' - \hat{\theta}_m) ,\quad(4c)$$

$$\hat{\mu}_2'(t) = \sum_{n=-N+1}^{N}\sum_{m=1}^{M} c_{n,m}\sin(2\pi f_n t - \theta_m' - \hat{\theta}_m) ,\quad(4d)$$

where N-by-M denotes the number of sinusoids, determining the realization expenditure and the performance of the resulting channel simulator. The phases $\hat{\theta}_m$ are uniformly distributed random variables, which can be obtained simply by means of a random generator with uniform distribution over the interval $(0, 2\pi]$. The so-called Doppler coefficients $c_{n,m}$, discrete Doppler frequencies f_n, and phases θ_m (θ_m') are simulation model parameters, which have to be determined in such a way that the statistical properties of $\hat{\mu}_i(t)$ and $\hat{\mu}_j'(t)$ are matching those of the stochastic processes $\mu_i(t)$ and $\mu_j'(t)$ ($i,j = 1,2$), respectively, as good as possible. By using the method of exact Doppler spread [17], we get the following closed-form expressions:

$$c_{n,m} = \frac{\sigma_0}{\sqrt{NM}} ,\qquad(5a)$$

$$f_n = f_{max}\sin\left[\frac{\pi}{2N}\left(n - \frac{1}{2}\right)\right] ,\qquad(5b)$$

for $n = -N+1, -N+2, \ldots, N$ and $m = 1, 2, \ldots, M$. According to a new computation method proposed in the Appendix, we can derive the following expressions

$$\theta_m = 2\pi F_1\varphi_m ,\qquad \theta_m' = 2\pi(F_1+\chi)\varphi_m ,\qquad(6a,b)$$

with

$$\varphi_m = \alpha\ln\left(\frac{1}{1 - \frac{m-1/2}{M}}\right)\qquad(7)$$

for $m = 1, 2, \ldots, M$. The above expressions (4)–(7) show us that the occurrence of a frequency hop $F_1 \rightarrow F_2$ of size $\chi = F_2 - F_1$ in the physical channel model corresponds to phase hops $\theta_m \rightarrow \theta_m'$ of sizes $2\pi\chi\varphi_m = \theta_m' - \theta_m$ ($m = 1, 2, \ldots, M$) in our simulation model, whereas the other parameters remain unchanged.

It is important to note that after calculating the quantities $c_{n,m}$, f_n, θ_m, and θ_m' with the above mentioned methods, these parameters are kept constant during simulation. However, the simulation model is still of stochastic nature, since the phases $\hat{\theta}_m$ are uniformly distributed random variables for all $m = 1, 2, \ldots, M$. Consequently, the processes $\hat{\mu}_i(t)$ and $\hat{\mu}_i'(t)$ are stochastic processes and the overall simulation model is also a stochastic model that can be used for the approximation and simulation of stochastic processes such as the above Rayleigh processes.

Fig. 1 shows the structure of the resulting stochastic continuous-time SFH Rayleigh fading channel simulator corresponding to the received envelope $\hat{\zeta}(t)$ with the carrier frequency F_1. By substituting in this figure the phases θ_m by θ_m', we can immediately obtain the model for the received envelope $\hat{\zeta}'(t)$ that corresponds to F_2.
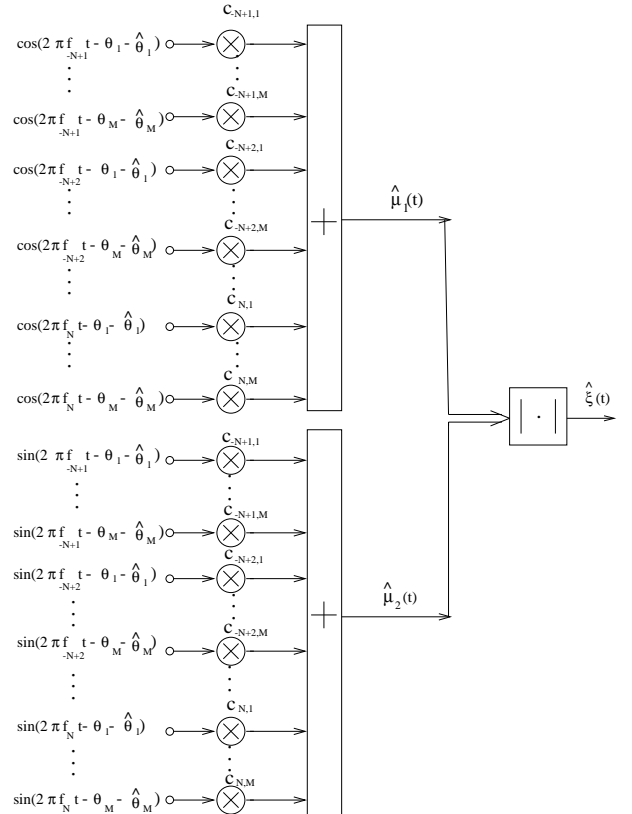

Fig. 1: SFH Rayleigh fading channel simulator.

Since all parameters of our stochastic simulation model are known quantities now, the counter parts of (2a) and (2b) can be calculated analytically by means of the following definitions:

$$\hat{r}_{\mu_i \mu_j}(\tau) := \lim_{T \to \infty} \frac{1}{2T} \int_{-T}^{T} E_{\hat{\theta}_m} \{\hat{\mu}_i(t)\hat{\mu}_j(t+\tau)\} dt \ , \qquad (8a)$$

$$\hat{r}_{\mu_i \mu_j'}(\tau, \chi) := \lim_{T \to \infty} \frac{1}{2T} \int_{-T}^{T} E_{\hat{\theta}_m} \{\hat{\mu}_i(t)\hat{\mu}_j'(t+\tau)\} dt \ , \quad (8b)$$

for all $i = 1, 2$ and $j = 1, 2$. Here, we take into account that different events $\hat{\theta}_m$ always result in different realizations for $\hat{\mu}_i(t)$ and $\hat{\mu}_j'(t)$. Therefore, we also consider the statistical average for all of these realizations with respect to $\hat{\theta}_m$. If we substitute (4a)–(4d) in (8a) and (8b), then we obtain the following relations after simple computations:

$$\hat{r}_{\mu_i \mu_i}(\tau) = \sum_{n=-N+1}^{N} \sum_{m=1}^{M} \frac{c_{n,m}^2}{2} \cos(2\pi f_n \tau) \ , \qquad (9a)$$

$$\hat{r}_{\mu_1 \mu_2}(\tau) = \hat{r}_{\mu_1' \mu_2'}(\tau)$$

$$= \sum_{n=-N+1}^{N} \sum_{m=1}^{M} \frac{c_{n,m}^2}{2} \sin(2\pi f_n \tau) \ , \qquad (9b)$$

$$\hat{r}_{\mu_i \mu_i'}(\tau, \chi) = \sum_{n=-N+1}^{N} \sum_{m=1}^{M} \frac{c_{n,m}^2}{2}$$
$$\cdot \cos(2\pi f_n \tau - 2\pi \varphi_m \chi) \ , \qquad (9c)$$

$$\hat{r}_{\mu_1 \mu_2'}(\tau, \chi) = -\hat{r}_{\mu_2 \mu_1'}(\tau, \chi) = \sum_{n=-N+1}^{N} \sum_{m=1}^{M} \frac{c_{n,m}^2}{2}$$
$$\cdot \sin(2\pi f_n \tau - 2\pi \varphi_m \chi) \ , \qquad (9d)$$

for $i = 1, 2$. Note that M has no influence on (9a) and (9b) if $c_{n,m}$ take the form of (5a), since $\sum_{m=1}^{M} \frac{1}{M} = 1$.

4. Numerical results and performance evaluation

In this section, we study the performance of the proposed SFH channel simulator by comparing the correlation properties of the simulation model [see (9a)–(9d)] with those of the reference model [see (3a)–(3d)].

1) Comparison of $\hat{r}_{\mu_i \mu_i}(\tau)$ with $r_{\mu_i \mu_i}(\tau)$: The substitution of (5a) and (5b) in (9a) results for $N \to \infty$ and $M \to \infty$ in

$$\lim_{\substack{N \to \infty \\ M \to \infty}} \hat{r}_{\mu_i \mu_i}(\tau) = \lim_{\substack{N \to \infty \\ M \to \infty}} \sum_{n=-N+1}^{N} \sum_{m=1}^{M} \frac{\sigma_0^2}{2NM}$$
$$\cdot \cos\left\{ 2\pi f_{max}\tau \sin\left[\frac{\pi}{2N}(n-\frac{1}{2})\right]\right\}$$

$$= \lim_{N \to \infty} \sum_{n=-N+1}^{N} \frac{\sigma_0^2}{2N}$$
$$\cdot \cos\left\{ 2\pi f_{max}\tau \sin\left[\frac{\pi}{2N}(n-\frac{1}{2})\right]\right\}$$

$$= \sigma_0^2 \frac{1}{\pi} \int_{-\pi/2}^{\pi/2} \cos(2\pi f_{max}\tau \sin z) dz$$

$$= \sigma_0^2 J_0(2\pi f_{max}\tau) = r_{\mu_i \mu_i}(\tau) \ . \qquad (10)$$

Thus, $\hat{r}_{\mu_i \mu_i}(\tau)$ tends to $r_{\mu_i \mu_i}(\tau)$ if $N \to \infty$ and $M \to \infty$. But even a limited number of sinusoids gives excellent approximation results for $r_{\mu_i \mu_i}(\tau) \approx \hat{r}_{\mu_i \mu_i}(\tau)$, as is demonstrated in Fig. 2 for $N = 20$ and $M = 20$. Note that we can reduce the number of parameters M without degrading the performance because M has no influence on $\hat{r}_{\mu_i \mu_i}(\tau)$.
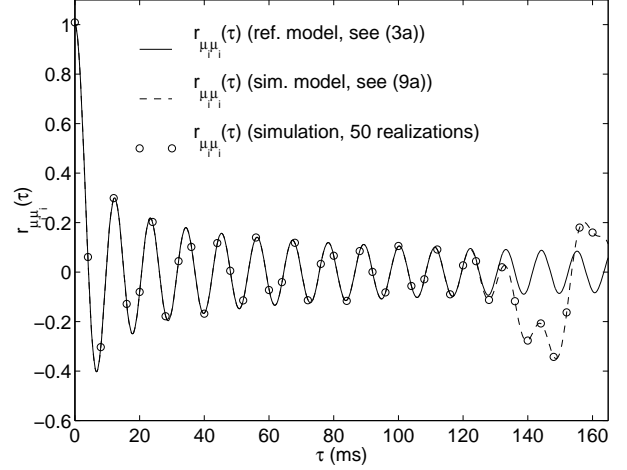
Fig. 2: Autocorrelation function $r_{\mu_i \mu_i}(\tau)$ (ref. model) in comparison with $\hat{r}_{\mu_i \mu_i}(\tau)$ (sim. model, $N = 20$, $M = 20$) for $f_{max} = 91$ Hz and $\sigma_0^2 = 1$.

2) Comparison of $\hat{r}_{\mu_1 \mu_2}(\tau)$ with $r_{\mu_1 \mu_2}(\tau)$: Substituting (5a) and (5b) in (9b) and letting $N \to \infty$ and $M \to \infty$ results in

$$\lim_{\substack{N \to \infty \\ M \to \infty}} \hat{r}_{\mu_1 \mu_2}(\tau) = \lim_{\substack{N \to \infty \\ M \to \infty}} \sum_{n=-N+1}^{N} \sum_{m=1}^{M} \frac{\sigma_0^2}{2NM}$$
$$\cdot \sin\left\{ 2\pi f_{max}\tau \sin\left[\frac{\pi}{2N}(n-\frac{1}{2})\right]\right\}$$

$$= \lim_{N \to \infty} \sum_{n=-N+1}^{N} \frac{\sigma_0^2}{2N}$$
$$\cdot \sin\left\{ 2\pi f_{max}\tau \sin\left[\frac{\pi}{2N}(n-\frac{1}{2})\right]\right\}$$

$$= \sigma_0^2 \frac{1}{\pi} \int_{-\pi/2}^{\pi/2} \sin(2\pi f_{max}\tau \sin z) dz$$

$$= 0 = r_{\mu_1 \mu_2}(\tau) \ . \qquad (11)$$

From this result, we realize that $\hat{r}_{\mu_1 \mu_2}(\tau)$ converges to $r_{\mu_1 \mu_2}(\tau)$ if $N \to \infty$ and $M \to \infty$. Actually, $r_{\mu_1 \mu_2}(\tau)$ and $\hat{r}_{\mu_1 \mu_2}(\tau)$ are exactly the same even with the reduced number of parameters N and M in case that M has no influence on $\hat{r}_{\mu_1 \mu_2}(\tau)$ and f_n [see (5b)] is a symmetrical function with respect to n, i.e., $f_{-N+1} = -f_N, \ldots, f_0 = -f_1$. Therefore, it follows that $\hat{r}_{\mu_1 \mu_2}(\tau) = r_{\mu_1 \mu_2}(\tau) = 0$ holds for all τ.

3) Comparison of $\hat{r}_{\mu_i \mu_i'}(\tau, \chi)$ with $r_{\mu_i \mu_i'}(\tau, \chi)$: The substitution of (5a), (5b), and (7) in (9c) results for $N \to \infty$ and

$M \to \infty$ in

$$\lim_{\substack{N \to \infty \\ M \to \infty}} \hat{r}_{\mu_i \mu_i'}(\tau, \chi) = \lim_{\substack{N \to \infty \\ M \to \infty}} \sum_{n=-N+1}^{N} \sum_{m=1}^{M} \frac{\sigma_0^2}{2NM}$$
$$\cdot \cos\left\{2\pi f_{max}\tau \sin\left[\frac{\pi}{2N}\left(n - \frac{1}{2}\right)\right]\right.$$
$$\left. -2\pi\alpha\chi \ln\left(\frac{1}{1 - \frac{m-1/2}{M}}\right)\right\}$$

$$= \lim_{N \to \infty} \sum_{n=-N+1}^{N} \frac{\sigma_0^2}{2N} \int_0^1 \cos\left\{2\pi\right.$$
$$\cdot f_{max}\tau \sin\left[\frac{\pi}{2N}\left(n - \frac{1}{2}\right)\right]$$
$$\left. -2\pi\alpha\chi \ln\left(\frac{1}{1-z}\right)\right\} dz$$

$$= \lim_{N \to \infty} \sum_{n=-N+1}^{N} \frac{\sigma_0^2}{2N} \int_0^\infty \frac{1}{\alpha} e^{-\frac{z}{\alpha}}$$
$$\cdot \cos\left\{2\pi f_{max}\tau \sin\left[\frac{\pi}{2N}\left(n - \frac{1}{2}\right)\right]\right.$$
$$\left. -2\pi\chi z\right\} dz$$

$$= \frac{\sigma_0^2}{\pi} \int_{-\frac{\pi}{2}}^{\frac{\pi}{2}} \int_0^\infty \frac{1}{\alpha} e^{-\frac{z}{\alpha}}$$
$$\cdot \cos\left(2\pi f_{max}\tau \sin y - 2\pi\chi z\right) dz\,dy$$

$$= \frac{\sigma_0^2}{\pi} \int_{-\frac{\pi}{2}}^{\frac{\pi}{2}} \int_0^\infty \frac{1}{\alpha} e^{-\frac{z}{\alpha}}$$
$$\cdot \cos\left(2\pi f_{max}\tau \sin y\right)$$
$$\cdot \cos\left(2\pi\chi z\right) dz\,dy$$

$$= \sigma_0^2 J_0(2\pi f_{max}\tau)$$
$$\int_0^\infty \frac{1}{\alpha} e^{-\frac{z}{\alpha}} \cos\left(2\pi\chi z\right) dz$$

$$= \frac{\sigma_0^2 J_0(2\pi f_{max}\tau)}{1 + (2\pi\alpha\chi)^2}$$

$$= r_{\mu_i \mu_i'}(\tau, \chi) . \tag{12}$$

From (12), we realize that $\hat{r}_{\mu_i \mu_i'}(\tau, \chi)$ converges in the two-dimensional (τ, χ)-plane to $r_{\mu_i \mu_i'}(\tau, \chi)$ if $N \to \infty$ and $M \to \infty$. But the quality of the achieved approximation $r_{\mu_i \mu_i'}(\tau, \chi) \approx \hat{r}_{\mu_i \mu_i'}(\tau, \chi)$ is good even for moderate values of N and M. Consider therefore Figs. 4(a) and 4(b), where on the basis of the COST 207 rural area profile [18] the numerical results of (3c) and (9c) are shown, respectively. To see more clearly how close our simulation model is in good conformity with the reference model, we also give the analytical and simulation results of $r_{\mu_i \mu_i'}(0, \chi)$ and $\hat{r}_{\mu_i \mu_i'}(0, \chi)$ for $N = 20$ and M=20 (see Fig. 5). Note that these functions represent the cross-correlation functions $\hat{r}_{\mu_i \mu_i'}(\tau, \chi)$ and $r_{\mu_i \mu_i'}(\tau, \chi)$ along the χ-axis, respectively.

4) Comparison of $\hat{r}_{\mu_1 \mu_2'}(\tau, \chi)$ with $r_{\mu_1 \mu_2'}(\tau, \chi)$: Substituting (5a), (5b), and (7) in (9d) and letting $N \to \infty$ and $M \to \infty$ gives us
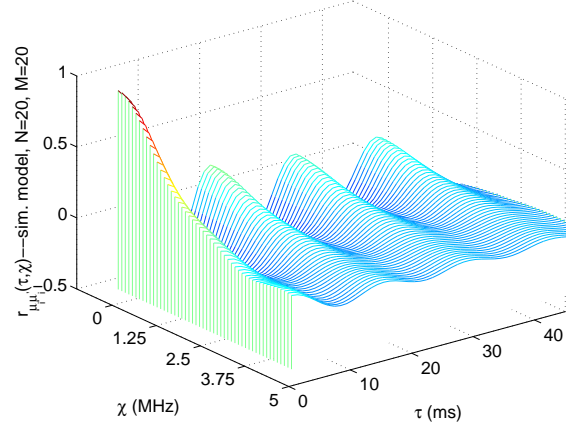

(a)
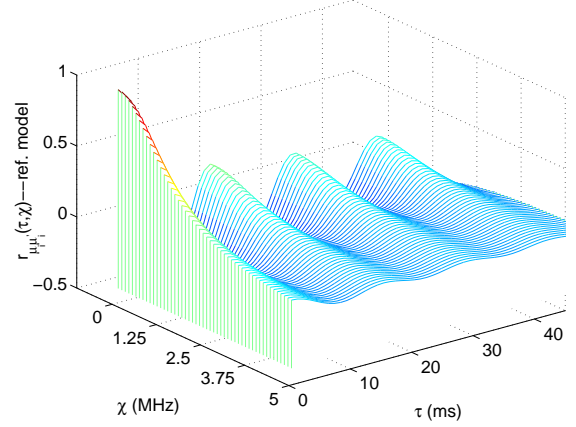
(b)

Fig. 4: Cross-correlation function $r_{\mu_i \mu_i'}(\tau, \chi)$ for the COST 207 rural area profile ($\alpha = 0.1086$ μs, $f_{max} = 91$ Hz, $\sigma_0^2 = 1$): (a) $r_{\mu_i \mu_i'}(\tau, \chi)$ (ref. model, cf. (3c)) and (b) $\hat{r}_{\mu_i \mu_i'}(\tau, \chi)$ (sim. model, $N = 20$, $M = 20$, cf. (9c)).
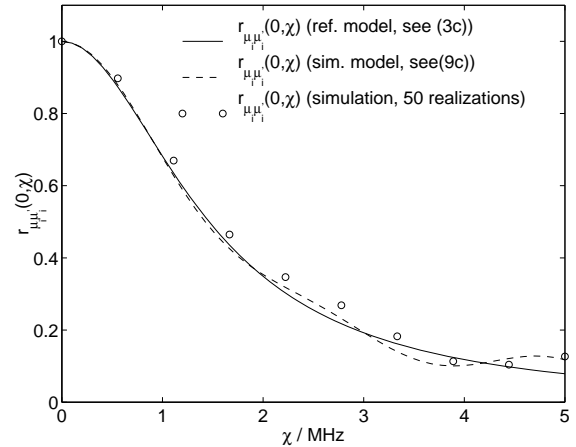

Fig. 5: Cross-correlation function $r_{\mu_i \mu_i'}(0, \chi)$ (ref. model) in comparison with $\hat{r}_{\mu_i \mu_i'}(0, \chi)$ (sim. model, N=20, M=20) for the COST 207 rural area profile ($\alpha = 0.1086$ μs, $f_{max} = 91$ Hz, $\sigma_0^2 = 1$).

$$
\begin{aligned}
\lim_{\substack{N\to\infty\\M\to\infty}} \hat{r}_{\mu_1\mu_2'}(\tau,\chi) &= \lim_{\substack{N\to\infty\\M\to\infty}} \sum_{n=-N+1}^{N}\sum_{m=1}^{M} \frac{\sigma_0^2}{2NM} \\
&\quad \cdot \sin\left\{2\pi f_{max}\tau\sin\left[\frac{\pi}{2N}\left(n-\frac{1}{2}\right)\right]\right. \\
&\quad \left. -2\pi\alpha\chi\ln\left(\frac{1}{1-\frac{m-1/2}{M}}\right)\right\} \\
&= \lim_{N\to\infty}\sum_{n=-N+1}^{N}\frac{\sigma_0^2}{2N}\int_0^1 \sin\{2\pi \\
&\quad \cdot f_{max}\tau\sin\left[\frac{\pi}{2N}\left(n-\frac{1}{2}\right)\right] \\
&\quad \left. -2\pi\alpha\chi\ln\left(\frac{1}{1-z}\right)\right\} dz \\
&= \lim_{N\to\infty}\sum_{n=-N+1}^{N}\frac{\sigma_0^2}{2N}\int_0^\infty \frac{1}{\alpha}e^{-\frac{z}{\alpha}} \\
&\quad \cdot \sin\left\{2\pi f_{max}\tau\sin\left[\frac{\pi}{2N}\left(n-\frac{1}{2}\right)\right]\right. \\
&\quad \left. -2\pi\chi z\right\} dz \\
&= \frac{\sigma_0^2}{\pi}\int_{-\frac{\pi}{2}}^{\frac{\pi}{2}}\int_0^\infty \frac{1}{\alpha}e^{-\frac{z}{\alpha}} \\
&\quad \cdot \sin\left(2\pi f_{max}\tau\sin y - 2\pi\chi z\right)dz\,dy \\
&= -\frac{\sigma_0^2}{\pi}\int_{-\frac{\pi}{2}}^{\frac{\pi}{2}}\int_0^\infty \frac{1}{\alpha}e^{-\frac{z}{\alpha}} \\
&\quad \cdot \cos\left(2\pi f_{max}\tau\sin y\right) \\
&\quad \cdot \sin\left(2\pi\chi z\right)dz\,dy \\
&= -\sigma_0^2 J_0\left(2\pi f_{max}\tau\right) \\
&\quad \int_0^\infty \frac{1}{\alpha}e^{-\frac{z}{\alpha}}\sin\left(2\pi\chi z\right)dz \\
&= -2\pi\alpha\chi\cdot\frac{\sigma_0^2 J_0\left(2\pi f_{max}\tau\right)}{1+(2\pi\alpha\chi)^2} \\
&= r_{\mu_1\mu_2'}(\tau,\chi)\,. \quad (13)
\end{aligned}
$$

Thus, $\hat{r}_{\mu_1\mu_2'}(\tau,\chi)$ tends to $r_{\mu_1\mu_2'}(\tau,\chi)$ if $N\to\infty$ and $M\to\infty$. As shown in Figs. 6(a) and 6(b), excellent approximation results for $r_{\mu_1\mu_2'}(\tau,\chi)\approx\hat{r}_{\mu_1\mu_2'}(\tau,\chi)$ can also be achieved even for moderate values of N and M. Concerning the behaviour of $r_{\mu_1\mu_2'}(\tau,\chi)$ and $\hat{r}_{\mu_1\mu_2'}(\tau,\chi)$ along the χ-axis, we compare $r_{\mu_1\mu_2'}(0,\chi)$ with $\hat{r}_{\mu_1\mu_2'}(0,\chi)$ for $N=20$ and M=20 in Fig. 7.

5. Conclusions

In this paper, we have proposed a novel stochastic channel simulator for the emulation of SFH Rayleigh fading channels. In particular, we have not only derived closed-form expressions for all parameters of the channel simulator, but also investigated the correlation properties of the simulation model from the analytical point of view. Furthermore, the performance of our simulation model with a limited number of parameters is evaluated by simulation of a typical GSM FH system. It is shown that the correlation properties of the proposed simulation model are in excellent conformity with the underlying reference model.
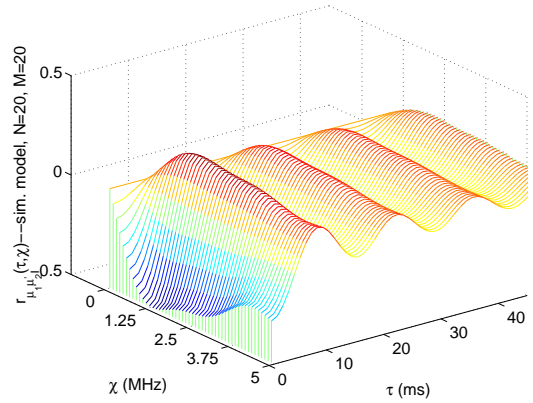
(a)
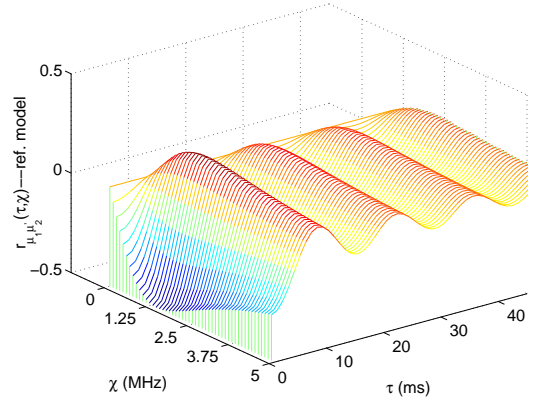
(b)

Fig. 6: Cross-correlation function $r_{\mu_1\mu_2'}(\tau,\chi)$ for the COST 207 rural area profile ($\alpha = 0.1086\ \mu s$, $f_{max} = 91$ Hz, $\sigma_0^2 = 1$): (a) $r_{\mu_1\mu_2'}(\tau,\chi)$ (ref. model, cf. (3d)) and (b) $\hat{r}_{\mu_1\mu_2'}(\tau,\chi)$ (sim. model, $N = 20$, $M = 20$, cf. (9d)).
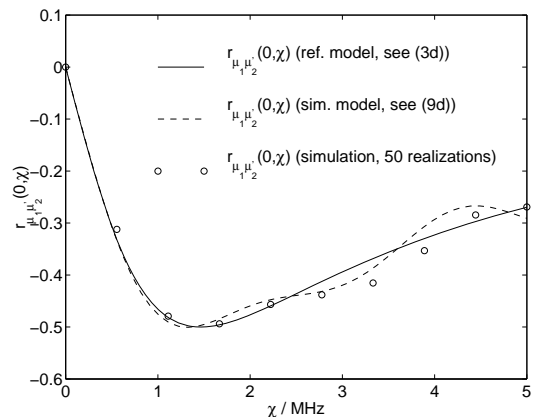

Fig. 7: Cross-correlation function $r_{\mu_1\mu_2'}(0,\chi)$ (ref. model) in comparison with $\hat{r}_{\mu_1\mu_2'}(0,\chi)$ (sim. model, N=20, M=20) for the COST 207 rural area profile ($\alpha = 0.1086\ \mu s$, $f_{max} = 91$ Hz, $\sigma_0^2 = 1$).

6. Appendix

In this Appendix, we present a new method to derive an explicit expression for the quantities $\varphi_m \geq 0$ in such a way that $\hat{r}_{\mu_i \mu'_i}(0, \chi)$ and $\hat{r}_{\mu_1 \mu'_2}(0, \chi)$ [see (9c) and (9d) for $\tau = 0$] are as close as possible to $r_{\mu_i \mu'_i}(0, \chi)$ and $r_{\mu_1 \mu'_2}(0, \chi)$ [see (3c) and (3d) for $\tau = 0$], respectively.

First, we derive φ_m by starting from $\hat{r}_{\mu_i \mu'_i}(0, \chi)$ and $r_{\mu_i \mu'_i}(0, \chi)$. By using (3c), (5a), and (9c), we obtain for the Fourier transforms of $r_{\mu_i \mu'_i}(0, \chi)$ and $\hat{r}_{\mu_i \mu'_i}(0, \chi)$ the relations

$$S_{\mu_i \mu'_i}(0, \varphi) = \frac{\sigma_0^2}{2\alpha} e^{-\frac{|\varphi|}{\alpha}} , \tag{14a}$$

$$\hat{S}_{\mu_i \mu'_i}(0, \varphi) = \frac{\sigma_0^2}{2M} \sum_{m=1}^{M} [\delta(\varphi - \varphi_m) + \delta(\varphi + \varphi_m)] , \tag{14b}$$

respectively. Now, we introduce intervals $I_m = (\varphi_{m-1}, \varphi_m]$ with $\varphi_0 = 0$ in such a way that (14a) and (14b) are related by

$$\int_{\varphi \in I_m} S_{\mu_i \mu'_i}(0, \varphi) d\varphi = \int_{\varphi \in I_m} \hat{S}_{\mu_i \mu'_i}(0, \varphi) d\varphi \tag{15}$$

for all $m = 1, 2, \ldots, M$. Then, we define an auxiliary function

$$G(\varphi_m) := \int_{-\infty}^{\varphi_m} S_{\mu_i \mu'_i}(0, \varphi) d\varphi , \tag{16}$$

which can be written by using (14b) and (16) as follows

$$\begin{aligned} G(\varphi_m) &= \frac{\sigma_0^2}{2} + \sum_{l=1}^{m} \int_{\varphi \in I_l} S_{\mu_i \mu'_i}(0, \varphi) d\varphi \\ &= \frac{\sigma_0^2}{2} + \sum_{l=1}^{m} \int_{\varphi \in I_l} \hat{S}_{\mu_i \mu'_i}(0, \varphi) d\varphi \\ &= \frac{\sigma_0^2}{2}(1 + \frac{m}{M}) . \end{aligned} \tag{17}$$

On the other hand, after substituting (14a) in (16), we obtain for the auxiliary function the expression

$$G(\varphi_m) = \frac{\sigma_0^2}{2}(2 - \exp(-\frac{\varphi_m}{\alpha})) . \tag{18}$$

Now, the quantities φ_m can easily be identified from (17) and (18) as

$$\varphi_m = \alpha \ln \left(\frac{1}{1 - \frac{m}{M}} \right) \tag{19}$$

for all $m = 1, 2, \ldots, M$. As shown in (7), we substitute on the right side of (19) the quantity m by $m - 1/2$ avoiding that $\varphi_m \to \infty$ when m=M.

Using the above method, the same result can be achieved for φ_m from the relation between $\hat{r}_{\mu_1 \mu'_2}(0, \chi)$ and $r_{\mu_1 \mu'_2}(0, \chi)$.

7. References

[1] Gass, J. H., and Pursley, M. B., "A comparison of slow-frequency-hop and direct-sequence spread-spectrum communications over frequency selective fading channels", IEEE Trans. Commun., 47(5):732–741, May 1999.

[2] Teh, K. C., Kot, A. C., and Li, K. H., "Multitone jamming rejection of FFH/BFSK spread-spectrum system over fading channels", IEEE Trans. Commun., 46(8):1050–1057, Aug. 1998.

[3] Kaleh, G. K., "Performance comparison of frequency-diversity and frequency hopping spread-spectrum systems", IEEE Trans. Commun., 45(8):910–912, Aug. 1997.

[4] Wu, T. C., Chao, C., and Chen, K., "Capacity of synchronous coded DS SFH and FFH spread-spectrum multiple-access for wireless local communications", IEEE Trans. Commun., 45(2):200–212, Feb. 1997.

[5] Cheun, K., and Choi, K., "Performance of FHSS multiple-access networks using MFSK modulation", IEEE Trans. Commun., 44(11):1514–1526, Nov. 1996.

[6] Halford, K. W., and Brandt-Pearce, M., "Performance of a multistage multiuser detector for a frequency hopping multiple-access system", Proc. 30th Annual Conference on Information Sciences and Systems (CISS), Princeton, New Jersey, USA, March 1996, pp605–610.

[7] Park, C. H., You, Y. H., Paik, J. H., Ju, M. C., and Cho, J. W., "Channel estimation and DC-offset compensation schemes for frequency-hopped bluetooth networks", IEEE Commun. Letters, 5(1):4–6, Jan. 2001.

[8] Steele, R., Ed., Mobile Radio Communications, IEEE Press, New York, 1995.

[9] Redl, S. M., Weber, M. K., and Oliphant, M. W., An Introduction to GSM, Artech House, Boston, 1995.

[10] Mehrotra, A., GSM system Engineering, Artech House, Boston, 1996.

[11] Lambrette, U., Fechtel, S., and Meyer, H., "A frequency domain variable data rate frequency hopping channel model for the mobile radio channel", Proc. IEEE 47th Veh. Technol. Conf., Phoenix, Arizona, USA, May 1997.

[12] Klingenbrunn, T., and Mogensen, P., "Modeling frequency correlation of fast fading in frequency hopping GSM link Simulations", Proc. IEEE 50th Veh. Technol. Conf., Amsterdam, The Netherlands, Sep. 1999.

[13] Pätzold, M., Laue, F., and Killat, U., "A frequency hopping Rayleigh fading channel simulator with given correlation properties", Proc. IEEE Int. Workshop on Intelligent Signal Processing and Communication Systems (IS-PACS), Kuala Lumpur, Malaysia, Nov. 1997.

[14] Rice, S. O., "Mathematical analysis of random noise", Bell Syst. Tech. J., 23:282–332, Jul. 1944.

[15] Rice, S. O., "Mathematical analysis of random noise", Bell Syst. Tech. J., 24:46-156, Jan. 1945.

[16] Jakes, W. C., Ed., Microwave Mobile Communications, IEEE Press, New Jersey, 1993.

[17] Pätzold, M., Killat, U., Laue, F., and Li, Y., "On the statistical properties of deterministic simulation models for mobile fading channels", IEEE Trans. Veh. Technol., 47(1):254-269, Feb. 1998.

[18] CEPT/COST 207 WG1, "Proposal on channel transfer functions to be used in GSM tests late 1986", COST 207 TD (86)51 Rev.3, Sep. 1986.